OPEN ACCESS

Direct-Contact Evaporation Using Different Refrigerants: A Review

Safaa Hafedh Hayder [1], Suad Hassan Danook [2], Hussein Sadiq Sultan [3],*

[1]*Department of HVAC Technical Engineering, North Technical University, Kirkuk, Iraq*
[2]*Department of Mechanical Engineering, North Technical University, Kirkuk, Iraq*
[3]*Department of Mechanical Engineering, College of Engineering, University of Basrah, Basrah, Iraq*
E-mail addresses: safaa.hafedh1982@gmail.com , Drsuadhassan2016@gmail.com , hussein.sultan@uobasrah.edu.iq

Abstract

The direct-contact evaporation method is characterized by its effectiveness in applications of heat exchangers, especially in cooling systems, due to the absence of any heat resistors that prevent the transfer of heat between the cold and hot medium. The direct contact heat transfer depends mainly on how quickly the heat is taken by the bubbles of the evaporative refrigerant from the liquid and the increase in its volume up to the top of the heat exchanger, which is usually a cylindrical liquid column so that the temperature drop therein is uniform and even. There is much research on the method of heat transfer by direct contact. In this research, we collected and summarized most of the theoretical and practical researches that examined this method with the most important findings.

© 2020 The Authors. Published by the University of Basrah. Open-access article.

Keywords: Direct-contact, evaporation; refrigerant.

1. Introduction

1.1. History of direct-contact cooling technology

The direct heat transfer technique between water and the cooling medium was first used in (1981) [1], where Stephan and Stopka used direct-contact evaporator. The direct heat transfer between hot water and cooling medium (R-C318), with diameters and different lengths. The diameter of the first pipe (D = 69 mm) and the length (L = 500 mm), while the diameter of the second pipe (d = 200 mm) and the length (L = 1200 mm).

The cooling technique was used by direct contact between air and water in air-washers systems used for cooling in dry zones. The air flow on the water spray evaporates the part of the water droplets and the heat from the other part of the droplet is absorbed, thus reducing the temperature of the air after its temperature is transferred to the cold part of water droplets.

1.2. Direct-contact heat evaporator

It is a tank in which water is kept stagnant or flowing according to the nature of the practical application of the system. The cold cooling medium flows from the bottom into

the water after leaving the expansion valve in the form of wet gas. The cooling medium receives heat from the water and evaporates completely and may turn into steamed steam. As the gases used in the cooling systems have a boiling temperature can reach below zero Celsius, and most of the cooling modes cannot be equated with water, so that the cooling medium can take the heat even if water at the natural temperature of the atmosphere temperature.
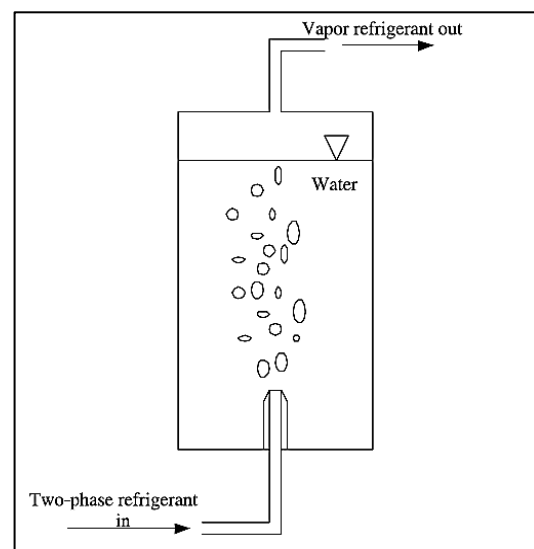
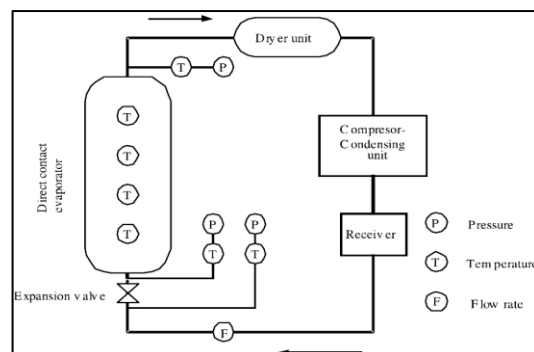

Fig. 1 Direct contact evaporator [2].

Fig. 2 Schematic diagram of the direct contact evaporation refrigeration system [2].

1.3. Direct-contact heat evaporator design

The evaporator is designed in the form of a cylindrical tank to be the heat absorption by the cooling medium evenly from all sides. It is best to stabilize vertically even when the bubbles of the cooling medium rise to the top when evaporated and are withdrawn by the cooling compressor and placed after the evaporator dryer absorbs water droplets to prevent it from reaching compressor.

The previous research that deals with the different applications of using the direct evaporative cooling method between the different cooling fluids and water have been reviewed, and previous studies and the extent of the developments in them will be reviewed according to the following main axes:

1. Study the water cooling and calculate the performance coefficient.
2. Study the volumetric heat transfer coefficient of heat transfer.
3. The study of the industrial ice production cold storage.
4. Study bubbles formation and the effect of the hydrate layer on cold storage.
5. Study bubbles formation and the effect of the hydrate layer on cold storage.
6. Studying the dimensionless relation of the Direct-Contact heat exchanger.

2. Study the water cooling and calculate the performance coefficient (COP)

Kiatsiriroat et al. in (1998) [3], developed the ice thermal energy storage having an injection of R12 refrigerant in the water by a direct contact heat exchanger. The water temperature drops to the freezing point and ice is created. The ice is utilized for producing chilled water for an air-conditioning aim. The system consists of a compressor, a condenser, an expansion valve, and a direct contact evaporator. This system has a capacity of about 2 tons of refrigeration. The system simulation performed from the mathematical model of every part has been taken out. It was determined that the performance of the cycle depends on two factors, the compressor speed and the mass flow rate of the refrigerant. The suitable states are 8-10 r.p.s for the compressor speed and 0.04-0.06 kg s^{-1} for the mass flow rate.
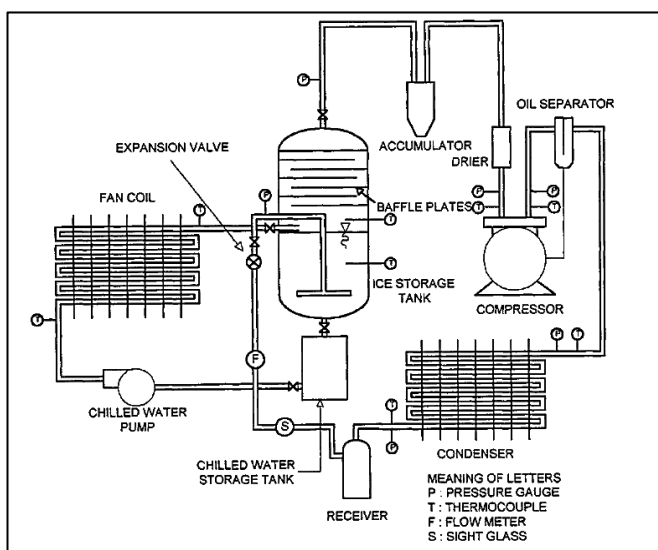
From the research experiment, it could be achieved that the method of direct contact heat transfer could present a high performance (COP = 3.4 - 3.6) with rapid refrigeration of the water and ice forming.
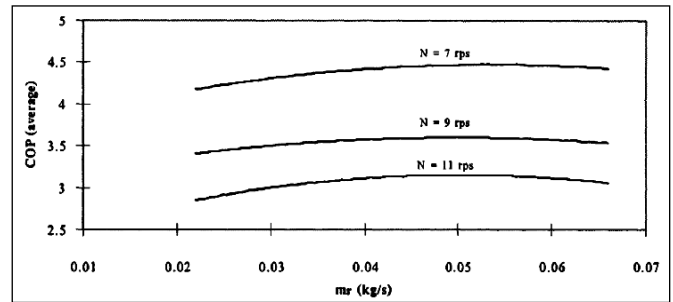

Fig. 4 The COP of the refrigeration system at various conditions.

Thitipatanapong in (2004) [4] studied the direct contact heat transfer in ice formation has been determined for the efficient ice production method of thermal energy storage for refrigeration purpose. It keeps constant thermal resistance throughout the ice formation process resulting in better heat transfer rate than the conventional ice-on-coil formation process. Furthermore, the direct contact heat exchanger (DCHE) can be utilized to produce ice slurry without any mechanical agitation. In this study, the probe experiment of pilot scale direct contact ice slurry production system with the capacity of ice formation of 2 tons of refrigeration is conducted. The thermal performances such as the volumetric heat transfer coefficient (Uv) and the coefficient of performance (COP) are examined. Moreover, the refrigerant HFC-134a is utilized as contact refrigerant in comparison with refrigerant CFC-12. The stream condition inside the DCHE is also examined. The supplies water is changed from 9.76 to 19.75 kg/m^{2}s, and the feed refrigerant is also changed from 0.98 to 2.19 kg/m^{2}s. Results explain that the ice formation temperature in HFC-134a system was 8.8 °C, and CFC-12 system was frozen at 4.0 °C. This is due to the variation in the physical properties of refrigerant called solubility of water as well as the Uv and COP for the HFC-134a system varied from 1.25 to 3.50 and from 150 to 250 kW/m^{3}K. Furthermore, the COP of CFC-12 system was about 2 and Uv changed from 55 to 100 kW/m^{3}K where the parameters were dependent on the stream conditions, which the high mass flow rate in refrigerant and water produced in high Uv and COP.

Figure 5 shows the experimental system setup. It was a normal direct contact heat exchanger with size Ø 300 mm and 1100 mm height, contained 40 kg of water as the phase change substance, combination on 3.5 ton refrigeration unit. Furthermore, the study of entire system performance utilizing CFC-12 gave the results in a relatively larger COP of the refrigeration unit, which was about 3.4 to 3.6. The performance of the direct contact evaporator, in expressions of heat transfer coefficient, depended on the mass flux of refrigerant. Table 1 shows the design information of DCHE, and Table 2 shows the main components of cooling system.
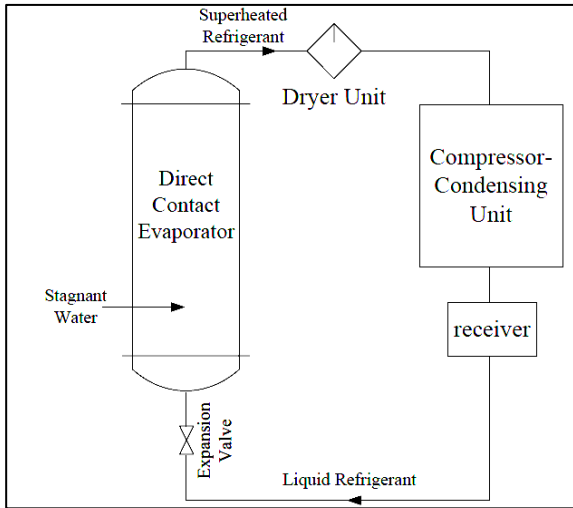

Fig. 3 Schematic diagram of the experimental set-up.

Fig. 5 Schematic diagram of experimental setup.

Table 1 The design information of DCHE.

Refrigerating capacity	7 kW$_{th}$
Operating temperature	-10 °C to 60 °C
Ice slurry concentration	30 %
Simulated heat load	7 kW$_{th}$
Operating time	Less than 2 hours

Table 2 the main components of cooling system.

Item	Description
Compressor	Hermetic type, MANEUROP MT64HM4CVE
Expansion device	DANFOSS, TE-2
Evaporator type	Flooded with compact brazed heat exchanger
Condenser	Shell & tube, water cooled
Capacity regulator	DANFOSS, KVC15
Refrigerant	HCFC-22

Figures 6 and 7 show the performance parameters namely, volumetric heat transfer coefficient (Uv) and coefficient of performance (COP) respectively. The first figure shows Uv in kW/m^{3}K during the ice formation process. It is apparent that the Uv in the HFC-134a system is larger than the CFC-12 system. The Uv were set between about 150 and 350 kW/m^{3}K for HFC-134a, but the results of CFC-12 remained constant at about 90 kW/m^{3}K. Then the second figure shows the COP of the refrigerator during the ice formation process. It is obvious that the COP had the same original of heat transfer rate, so the COP of HFC-134a was larger than the COP of CFC-12.
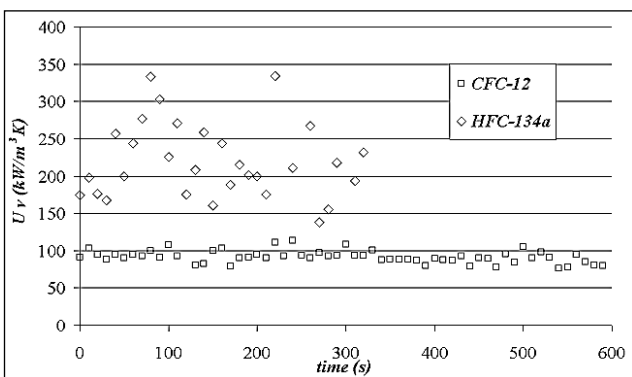

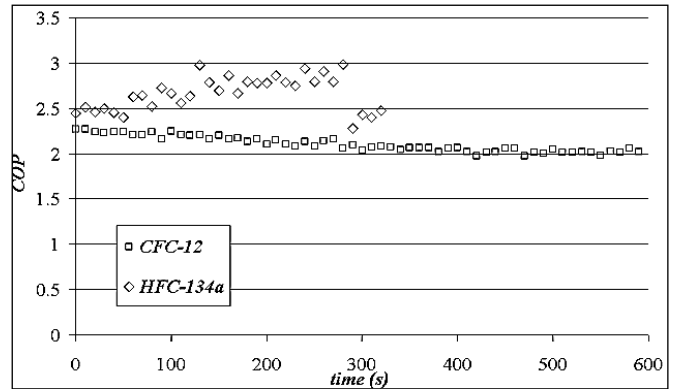**Fig. 6** The volumetric heat transfer with time.

Fig. 7 COP with time.

Figures 8 and 9 show the COP$_{avg}$ during the ice formation process, and the effect of mass flux on the LMTD. It is obvious that the COP$_{avg}$ had exactly the alike profile as Q$_{avg}$ due to the calculation in this test. The rise of refrigerant mass flow rate resulted in a rise of the COP$_{avg}$ from 1.25 to 3.00 as it directly changed the refrigeration capacity.
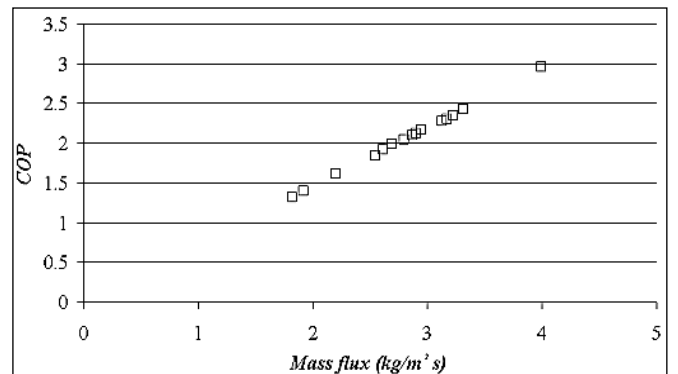

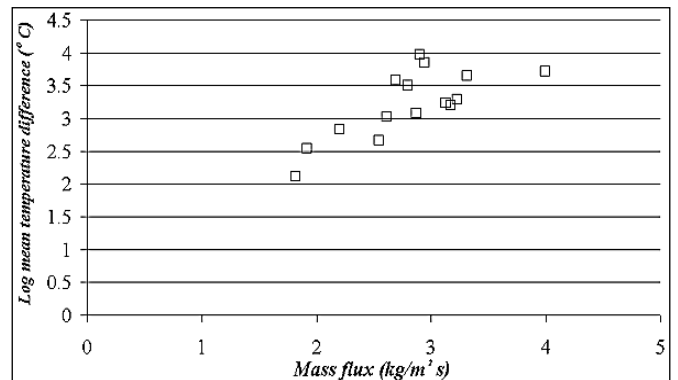**Fig. 8** COP and Refrigerant mass flux.

Fig. 9 LMTD and Refrigerant mass flux.

Ojimi, et al. in (2016) [5] studied experimentally the performance of a direct contact evaporation system utilizing R12 as a refrigerant. The process was performed by utilizing a direct contact evaporator, which is a tank containing a water column. The water vessel was refrigerated by injecting a refrigerant, R12, directly into the water. The refrigerant absorbed the heat required for evaporation from the water, causing the water to cool, or freeze, in proportion to the heat transferred between the two fluids. The experimental results explained that the process resulted in a reduction in water temperature to a lower boundary of temperature (12 °C), and may be reaching a freezing point in perfect states. The decrease in water temperature along the evaporator and the

performance coefficient of the evaporator are utilized as criteria to estimate the refrigeration system. By utilizing the heat balance concept between the heat extracted from the water and the electrical work COP was 4.86. Also, by considering an isentropic process for the experimental states, the theoretical COP was 7.7.

The technical specifications of the water refrigeration system depending on the requisite water inlet and exit temperatures, and the volumetric flux of water needed by the consumer. These specifications are utilized to estimate the capacity of the refrigeration coil (the evaporator), which is then utilized to size the remaining parts in the refrigeration system. The experimental setup consists of:

1. Evaporator (direct contact).
2. Drying unit.
3. Compressor.
4. Condenser.
5. Expansion valve.
6. The refrigerant.
7. The bowl receiver gases.

The water is refrigeration by injecting refrigerant into the pot gases throughout the expansion valve to reduce pressure and temperature. This underscores the importance of the valve is not only controlling the cooling rate, but also the pressure and temperature of the refrigerant. The cooling will be in two stages: the first stage is to inject refrigerant, and the second stage is lowering the water temperature to the freezing point by transferring heat to the refrigerant, which turns to steam and flows out of the storage tank to the compressor and then to the condenser. Before the refrigerant passes to the compressor, it must dry by passing through the drying unit. The basic function of the drying unit is to extract moisture from the two-phase steam to protect the compressor from damage. Fig. 10 shows a schematic diagram of the system.
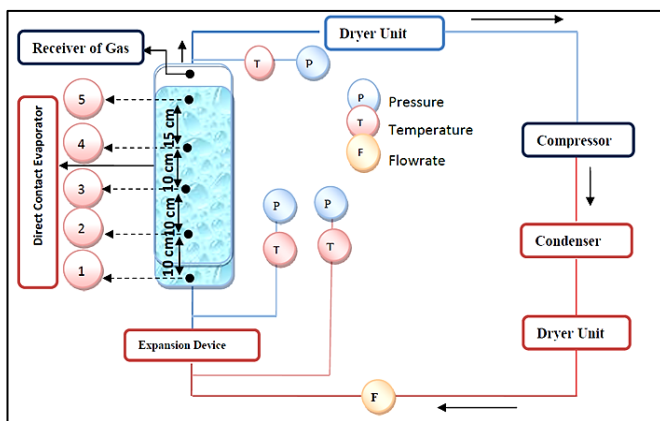

Fig. 10 Schematic diagram of the experimental apparatus.

The relation below represents the coefficient of performance of the system (COP) [6, 7, 8] as the evaporator heat ($Q_{evap.}$) divided by the compressor work ($W_{comp.}$), both measured in (kJ). The experimental coefficient of performance is calculated by dividing the quantity of heat that removed from the water to the electric work utilized in the compressor, as follows:

$$Q_{cooling} = m \, C_p \, (T_{t=0} - T_{t=1.8\ hour}) \qquad (1)$$

The coefficient of performance (COP) for the system calculated as follow:

$$COP = \frac{Q_{cooling}}{W_{compressor}} \qquad (2)$$

And,

$$Compressor\ Work\ = I \times V \qquad (3)$$

Where, I: is the current (A).

V: is the voltage (v).

The theoretical COP for the cycle is estimated by applying measured values of pressure and temperature from the system:

$$COP = \frac{Q_{Evap.}}{W_{compressor}} \qquad (4)$$

According to the experimental results, it is clear that throughout the period of work (approximately 1.6 hours) there was a clear reduction in the temperature of the water about (13 °C), as a result of heat absorption by refrigerant. The decrease in temperature of the storage vessel (evaporator), which is considered to be an isolated and adiabatic process, is equal to 13 °C at most points. This gives the effectiveness of the direct contact evaporator for refrigeration. It is possible that the drop in the temperature of the evaporator may rise if the quantity of refrigerant is increased. In addition, this will likely increase the time required to complete.

Similar behavior of all five curves that clear in the results showed that there was no significant effect of the position (of measured temperature) and the measured pressure on the process but the time plays the significant part in the test. Effect of another factor can be studied and it presents different results for the process.

It is noted from the coefficient of performance estimations, that the coefficient of performance of the cycle (COP = 7.7) is relatively high compared to traditional cycles, which reach approximately 4 [9]. This explains that the process is not only feasible but also highly efficient.

Zhang et al. in (2019) [10] studied the direct contact ice formation technique, ice blockage around the injector, high coolant charge and difficulty in separating the coolant from water always occur. In order to overcome these problems, the combined of a spiral jet (SPJT) and a horizontal PVC pipe is developed to provide continuous ice production, and RC318 is chosen as the coolant. The effect of rotational speed of the compressor on water temperature decrement, ice production rate, ice packing factor (IPF), COP and coefficient of ice producing performance (CIPP) is examined in this study.

The results present that as the rotational speed increases, a faster reduction of water temperature and a higher ice production rate are determined, which result in higher IPF under constant duration. However, a rise in rotational speed leads to a drop in COP. The maximum CIPP is 6.64×10^{-3} kg/kJ at the rotational speed of 2700 rpm. Moreover, at the high rotational speed of 2820 rpm, the refrigeration capacity becomes worse at the later stage of ice production process. Conclusively, the rotational speed of 2700 rpm is considered as the optimal working condition.

Figure 11 the experimental set-up which consists of a direct contact heat exchanger (DCHE), an SPJT, an ice slurry storage tank, a compressor, a plate heat exchanger, an expansion valve and a water chiller. The DCHE is a

horizontal PVC pipe with 3 m length and 45 mm inner diameter. An SPJT is inserted at the entry of the horizontal PVC pipe. The physical diagram of the SPJT is given in Fig. 12 whose type is SPJT JJCO1/2 120 316L. The ice slurry storage vessel is composed of two connected carbon steel vessels, which are both 80 cm diameter and 130 cm length. Two sight glasses are fixed on both sides of the upper vessel for observing inside aspect.
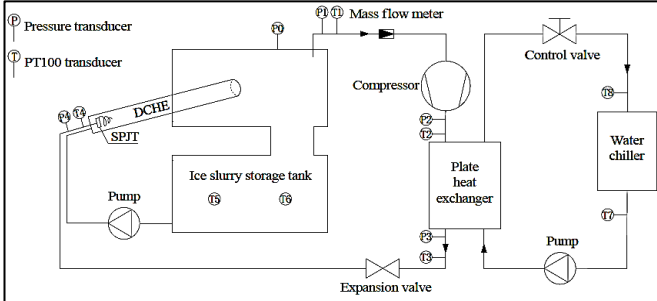

Fig. 11 Schematic diagram of the experimental.

Fig. 12 Physical photo of the SPJT.

During ice formation period, the water temperature does not change at its freezing point and the mass of ice during a time interval can be calculated from equation (5):

$$m_{ice} = \frac{mr\,(h_{ro} - h_{ri})}{r_w} \,\Delta t_{ice} \tag{5}$$

Where, r_w is latent heat of freezing of water, 335 kJ/kg. Even though system at 2700 rpm rotational speed shows slightly 0.86 % lower COP than that at 2580 rpm, the CIPP of system at 2700 rpm rotational speed is higher than that at 2580 rpm. Furthermore, the average ice production rate at 2700 rpm rotational speed is 14.37 % faster than that at 2580 rpm, indicating that more ice can be produced at the same duration at 2700 rpm. In general, system at 2700 rpm rotational speed shows the best performance.

As for the CIPP of the RC318 ice formation system, as tabulated in the following table, the system gives high CIPP by up to 0.15 % and 8.32 % at the 2700 rpm rotational speed in comparison with that at 2580 rpm and 2820 rpm, respectively.

Even though the system gives slightly 0.86 % lower COP at 2700 rpm rotational speed than that at 2580 rpm, the CIPP of the system at 2700 rpm rotational speed is larger than that at 2580 rpm. Furthermore, the average ice product rate at 2700 rpm rotational speed is 14.37 % faster than that at 2580 rpm, showing that more ice can be produced at the same duration at 2700 rpm. In general, the system gives the best performance at 2700 rpm rotational speed.

Table 3 the system performance parameters for various rational speeds of the compressor.

Rotational Speed	2580 (rpm)	2700 (rpm)	2820 (rpm)
The average cooling capacity (kW)	11.37	12.89	13.89
The average COP	2.32	2.30	2.12
The average CIPP (10-3 kg/kJ)	6.63	6.64	6.13

3. Study the volumetric heat transfer coefficient of heat transfer

Stephan and Stopka in (1981) [1] studied direct heat transfer between hot water and cooling medium (R-C318) was used with different diameters and lengths. The diameter of the first tube (d = 69 mm) and the length (L = 500 mm), while the diameter of the second tube (d = 200 mm) and length (L = 1200 mm). The volumetric heat transfer coefficient between the liquid was calculated by:

$$\overline{kv} = \frac{\dot{Q} + \Delta\dot{m}_r\,r_w}{V\,\Delta T_m} \tag{6}$$

And the mass flow rate of water vapor ($\dot{m}_w^g$):

$$\dot{m}_w^g = \frac{p_w\,(T_{w2})\,M_w}{p_r\,(T_{rs})\,M_r}\,\dot{m}_r^g \tag{7}$$

It was found that its value was 40 times higher than conventional cooling methods. A simplified model has been developed with respect to heat transfer around each drop of the cryogenic fluid. It was concluded that the theoretical calculations were practical. Figure 13 illustrates the relationship of volumetric heat transfer coefficient with mass flow ratio.
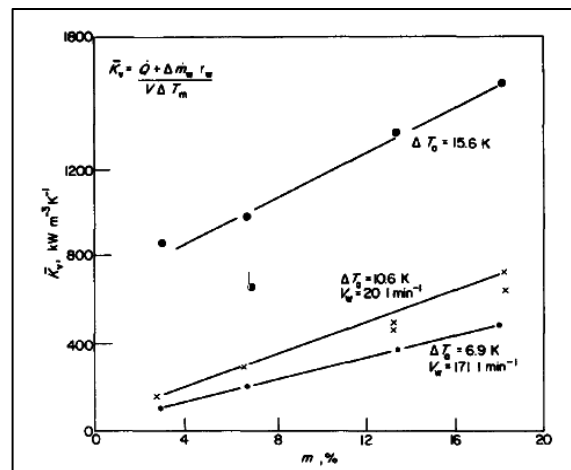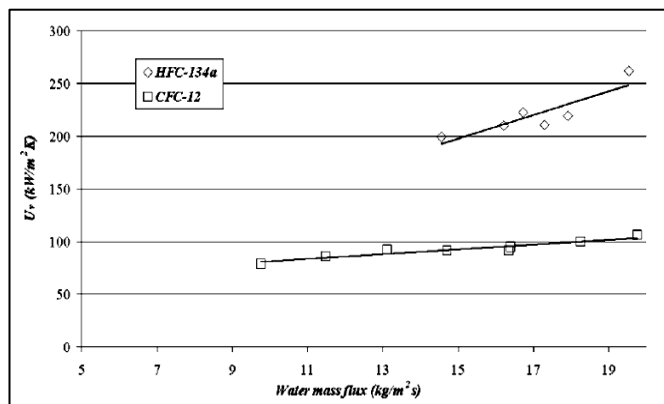

Fig. 13 Volumetric heat transfer coefficient with mass flow ratio.

They are good at predicting practical results. The model relies on the integration of heat transfer properties for you into a single bubble with the water movement of the two-phase flow. Thus, performance is expected to be good for direct-evaporation. The results were as shown in the following table:

Table 4 the Comparison of experimental values of h_v.

	Sideman and Gat	Blair et al.	Present Expt.
Dispersed phase	n-pentane	refrigerant-113	cyclopentane
Specific gravity	0.63	1.55	0.68
Enthalpy of vaporization (J/kg)	3.57×10 s	1.47×10 s	4.19×10 s
Continuous phase flow Rate (kg/min)	1.295	1.370	0.0
Dispersed phase flow Rate (kg/min)	0.042	0.101	0.257-0.386
h_u watts/m³ °C	$18 \times 10"$	$12.2 \times 10"$	$4.52-6.0 \times 10"$

Thitipatanapong et al. in (2003) [8], studded the direct-contact heat transfer in ice formation. The refrigerant HFC-134a has been used as contact refrigerant in comparison with refrigerant CFC-12. In this experiment, the test study of ice slurry formation on pilot scale direct-contact heat exchanger was conducted with the capacity of ice formation of 1.5 refrigeration ton. The supplies water for ice slurry production has a mass flux in direct contact vertical cylinder changing from 9.76 to 19.75 kg/m²s. The results explain evaporating temperatures during each ice slurry formation process at 8 °C for HFC-134a and 4 °C for CFC-12. The volumetric heat transfer coefficient of HFC-134a is larger than that of CFC-12.

Fig. 14 The average volumetric heat transfer coefficient VS feed water mass flow rate in comparison of CFC-12 and HFC-134a.

3.1. Effect of refrigerant types

In this test, CFC-12 and HFC-134a were chosen. These refrigerants have several similarities due to the replacement of phasing-out CFC-12 with HFC-134a.

Table 5 the test results of several variations in performance parameters.

	CFC-12	HFC-134a
Water mass flux (kg/m²s)	16.35	16.20
Average $LMTD_{DCHE}$ (°C)	5.85	3.46
Freezing temperature (°C)	4.0	8.8
Evaporation pressure during freezing (MPa$_{abs}$)	0.35-0.31	0.51-0.37
Average volumetric heat transfer coefficient (kW/m³K)	91.62	209.7
Ice slurry solution temperature in the storage tank (°C)	4.5	10.0

The experiments show that HFC-134a has relatively higher volumetric heat transfer coefficient than CFC-12 as shown in Fig. 2. This may cause from water solubility of refrigerant. The higher water solubility refrigerant such as HFC-134a has relatively higher volumetric heat transfer coefficient. The volumetric heat transfer coefficient of HCFC-22, which is high water soluble, is higher than CFC-12, which is less water soluble.

Thitipatanapong and Limmeechokchai in (2004) [11] investigated an examination pilot scale of a direct contact heat exchanger (DCHE) for ice slurry production was fabricated and evaluated. The study investigated the DCHE of Ø 114 mm and 1000 mm height utilizing evaporated refrigerant as a disperse phase and solidified water as a continuous phase. The heat transfer rate into the DCHE was changed between 3.0 and 6.5 kW, while the water flow rate across a heat exchanger was changed, and its inlet temperatures were controlled at 13 °C and 15 °C. As a result, the freezing point variation of the ice-water solution was found to be 7.95 °C. Moreover, the first law of thermodynamic indicated that the DCHE could be considered as a theoretically adiabatic mixing vessel. The mean temperature difference for the DCHE (MTD) shows that the stream conditions of water and refrigerant flow across the heat exchanger absolutely change on the system performance.

In this study, an experimental DCHE is analyzed utilizing the adiabatic mixing vessel mode as the reference to the ideal condition. Furthermore, the working fluids utilized in the DCHE are evaporated HFC-134a as a disperse phase and solidified water as a continuous phase, and the supplies water to DCHE was managed at 13 °C and 15 °C.

The main component of the system is DCHE, where the water and the refrigerant are mixed and transferred heat to each other to produce ice, which has 114 mm (4 inches) nominal diameter stainless steel pipe with 1100 mm height, 11 liters of volume, and the refrigerant mass flow rate inside changes from 1.5 to 3.2 kg m^{-2}s^{-1}, which follows to heat transfer rate from 3.0 to 6.5 kW. Moreover, the water mass flow rate changes from 8.0 to 14.5 kg m^{-2}s^{-1}. At its bottom, there are two inlet ports; the refrigerant passes through the distributor from the bottom while the water goes into the DCHE from the sideway port over distributor as shown in the Fig. 15.
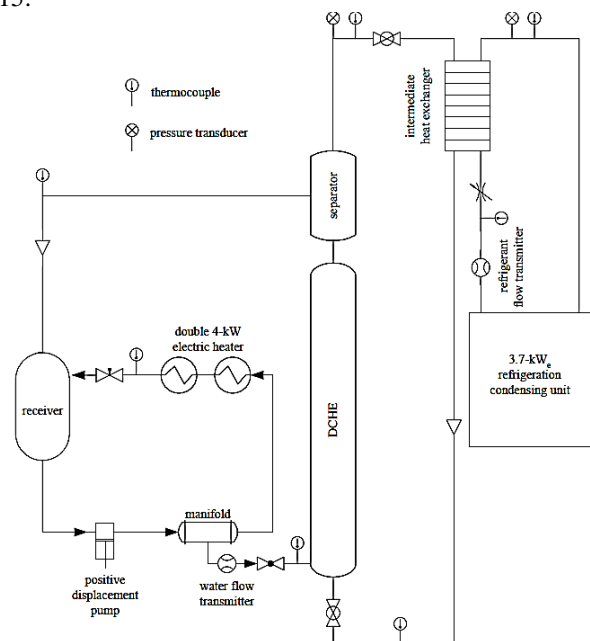
Fig. 15 Schematic diagram of experimental setup.

The mean temperature difference (MTD) as a significant key parameter of the heat exchanger is utilized to describe the average temperature difference between hot and cold fluids especially for latent heat transfer in this heat exchanger. As the refrigerated stream in this application is evaporation which is constant temperature heat transfer process, so the mean temperature of the cold stream is equal to the saturation temperature of cooling at operating pressure as shown in the following equation:

$$MTD = \left| \frac{(T_{w,\,out} + T_{w,\,in})}{2} \right| \qquad (8)$$

The study indicated utilizing the comparison of the temperature difference between the ice-water solution exit and the refrigerant exit as shown in the Fig. 16 that inclined solid line presents ideal adiabatically mixing and the dash lines in top and bottom indicate ± 10 % different from the ideal. The concern in the figure, most of the experimental results lied within ± 10 % of error so it could have been concluded that heat exchanger operated nearly to the ideal condition, which sometimes is assumed as the uneconomically excess structure of the heat exchanger.
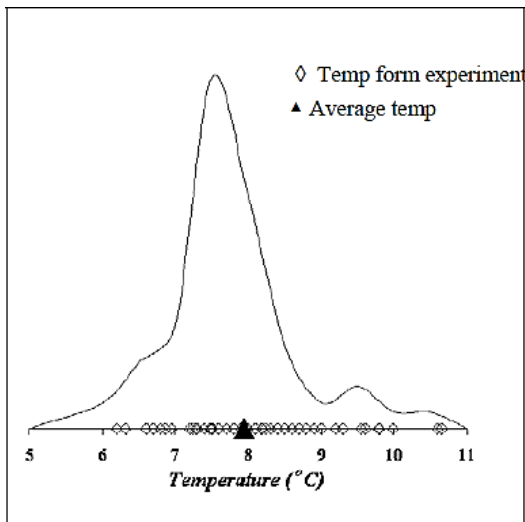

Fig. 16 Distribution curve of ice-water solution temperature.
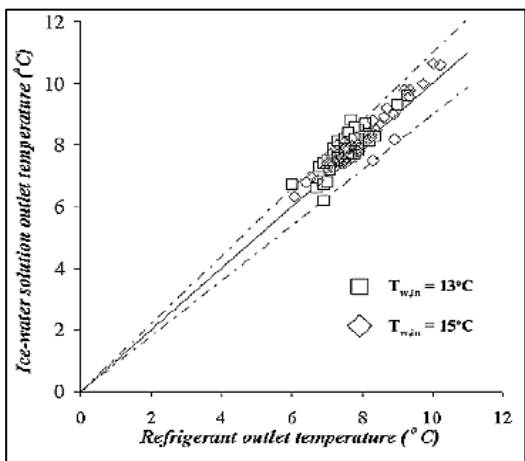

Fig. 17 Comparison of temperature at outlet between both streams.

Although the first law of thermodynamic analysis explained that the system for all fluid stream condition

operated near to theoretical condition, the further parameter, the mean temperature difference (MTD), explained that the DCHE performances depended on the fluid stream condition crossed the heat exchanger, as shown in the Fig. 18.
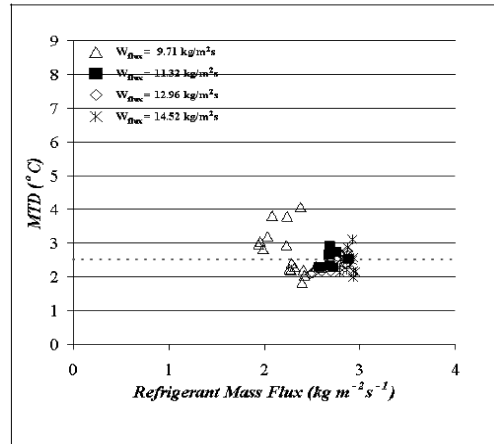
(a) at $T_{w.in}$ = 13°C
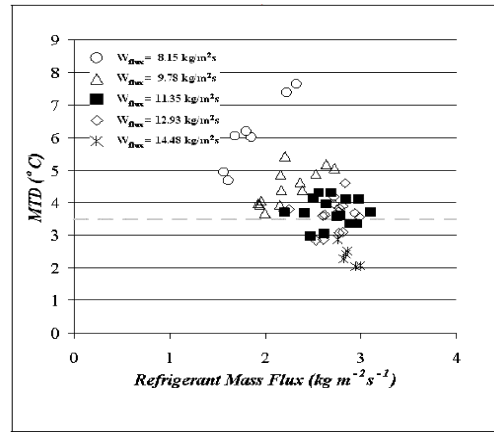
(b) at $T_{w.in}$ = 15°C

Fig. 18 Mean temperatures (MTD) vs. refrigerant mass flux at various water mass fluxes. (a) at $T_{w.in}$ (13 °C), (b) at $T_{w.in}$ (15 °C).

Jassim and Abdulkhaleq in (2014) [12] presented investigation deals with the empirical study of three-phase direct-contact heat exchanger, for Water-Freon R11 system, where water is the continuous phase (liquid) and Freon R11 (liquid-gas) is the dispersed phase.

The experiment section consisted of a cylindrical Perspex column with inner diameter 8 cm and 1.2 m long, in which, water was to be confined. Liquid Freon R11 droplets were injected into the hot water filled column, through a special design of distributors at the bottom of the column. The liquid Freon R11 drops rose on their way up and evaporated into two-phase bubbles at atmospheric pressure. The study was devoted to express the effect of process variables such as column height, Freon R11 mass flow rate and initial temperature of water on the average percentage holdup, heat transfer rate, volumetric heat transfer coefficient, and effectiveness.

The collected experimental results explained that the average percentage holdup increased with increase in the process variables. The heat transfer rate increased clearly with an increase in the mass flux of Freon R11, while I increased very little when column height and initial temperature of water increased, it increased two times when increasing the mass flux from 1.8 to 5.4 kg/hr. The volumetric heat transfer coefficient was determined to decrease with an increase in column height and initial temperature of water, while it was increased with an increase

in mass flow rate of Freon R11. The effectiveness was determined to increase (maximum 90 %) with increasing in column height and decreasing in the mass flux of Freon R11 and initial temperature of water. Statistical analysis was performed to get general correlations for the average percentage holdup, heat transfer rate, volumetric heat transfer coefficient and effectiveness as a function of the examined parameters.

The correlation relation for the plotted test results are done to know the process variables effect on the average percentage holdup, heat transfer rate, volumetric heat transfer coefficient, and exchanger efficiency. These relations are made by utilizing the curve fitting method. This fitting is done by Data Fit program version 9. The form of these relationships is:

$$\Pi = \alpha * H^{\beta} * \dot{m_d} * \Delta T^{\delta} \tag{9}$$

From the analysis, the following conclusions are made:
1. The average percentage holdup increases with increasing in the process variables and distributor geometry except with inlet temperature of Freon R11 it is decreased. Its maximum increase is 85 % when the column height increases from 5 to 40 cm.
2. The heat transfer rate increase clearly two times when increase the mass flow rate of Freon R11 from 1.8 to 5.4 kg/hr.
3. The volumetric heat transfer coefficient is affected with change in the column height and mass flow rate of Freon R11 and its maximum value will be at lower column height and higher mass flow rate.
4. The effectiveness increases (maximum 90 %) when the column height increase and the initial temperature of water decrease.

4. The study of the industrial ice production cold storage

Isobe and Mori in (1992) [13] experimented the refrigerated storage by evaporation of HFC-134a (CH2FCFs) or HCFC-123 (CHCl2CF3) produced into direct contact with water in a crystallizer, which was organized into a vapor compression refrigerator circle. The degree of sub-cooling before the inception of the gas-hydrate formation with HFC-134a was located to be decreased by the increasing of powdery alumina or zinc or the increasing of a surfactant to the water, while the addition of Pseudomonas fluorescents, a strain of ice-nucleating bacteria, explained no effect. The use of HCFC-123 instead of HFC-134a produced in the formation of slush ice only; no sign of gas-hydrate formation was verified. The purpose of this is supposed to lie in the molecular dimension of HCFC-123.

The setup was a small vapor pressure cooler that included a crystal (i.e. storage container of gas hydrates) as an option to conventional evaporators. The crystalline was a cylindrical column with a vertical adjustment and was covered with a vacuum, with an inner diameter of 80 mm and a height of 600 mm. Before each experimental operation, the crystalline was charged by 600 cm 3 of demonized water and extracted and heated from outside to the temperature rose to 30 °C or higher. This heating was done to assure that a small quantity of previously formed gas or ice hydrates could be eliminated and that they could serve as nuclei in the successful experimental range, i.e. the refrigeration process. The operation started when refrigerant (HFC-134a or HCFC-123),

mostly in the liquid phase, was carried into the crystal into a bottom entry to partly evaporate and creating a liquid layer a few centimeters under a pool of water. The radiator was filled to the crystallization apparatus at a constant rate to compensate for the flow from the top of the refrigeration column of the refrigerant produced by heat transfer of the radiator, causing the refrigeration of the entire contents of the crystallization to the start of the hydrate or formation of the ice. Once the hydrate is formed, the liquid bottom layer of the radiator acts as a summary buffer against the pressure variations in the column due to the speedy installation of the coolant as guest particles in the hydrate.

Table 6 Sub-cooling (temperature down from the breakdown temperature 9.9 °C) in the bulk of water at the beginning of gas-hydrate formation with HFC-134a.

Additives	Amount per cubic cm of water	Super-cooling (~95 % converge) (k)
None	-	12.3 ± 1.6
Alumina (#40-80)	1.67 mg	9.5 ± 1.7
Zinc (#40-80)	1.67 mg	9.8 ± 1.4
Pseudomonas fluorescens	0.167 mg	12.9 ± 2.4
Zonyl Fluorosurfactant	1.0 mm³	8.5 ± 1.8
Unidyne DS-401	1.0 mm³	8.0 ± 1.7

5. Studying the effect the amount and velocity of refrigeration injection

Celata et al. in (1995) [6] investigated experimentally the direct contact boiling of immiscible liquids. The continuous state, water, is under stagnant situations, while the dispersed one, Freon 114, is injected in the experiment section with various velocity and thermodynamic situations through a nozzle. The injection device has been designed to change the quantity of injected refrigerant and/or liquid injection velocity.

The experiment section is a Plexiglas vertical cylinder 72 mm i.d., 2.0 m long. Test data are taken from high-speed movies of the continuous phase level through and after the Freon 114 injection, as well as from the movies of the rising boiling dispersed phase (injected under nearly saturation conditions). Evaporation rate has been described as a purpose of thermal-hydraulic conditions (i.e. water temperature, operation pressure, and Freon mass flow rate). Direct contact boiling efficiency was derived by the evaluation of the fraction of Freon that did not undergo the boiling process during the transit in the test section.

Table 7 the experimental runs were given out as a combination of the following values.

R 114 inlet temperature, $T_{d,in}$ (nearly saturated)	17, 20, 23, 25, 30 °C
Water superheating, T_w- $T_{d.sat} = \Delta T_s$	10, 13, 15, 17, 20, 25 K
R 114 injection velocity, u_n	from 0.56 to 1.8 m s
Injected volume of R 114, $V_{od,1}$	from 1.5 to 3 cm 3
System pressure, $p_\infty = P_{sat}(T_{d,in})$	from 0.16 to 0.25 MPa

From a preceding study of the jet evolution, performed with the square channel experiment section, continuous injection of R 114 and a digital picture processing of vapor bubbles, the jet was adopted to break into bubbles only in the proximity of the injection point. The four images are taken

1/7 s after each other. Jet evolution in the round duct experiment section verifies the assuming of the quick fragmentation into droplets of the liquid jet. It is therefore thought important to schematize the jet evolution in the water cylinder as a series of drops increasing independently of each other. The study of the jet boiling may, therefore, be applied to the evaluation of the variation between the actual behavior (the experimental one) and the ideal behavior of a set of isolated single drops. On the other hand, it will be important to estimate all possible aspects characterizing the actual behavior with regard to the ideal one. As for any drop, it is possible to determine the total evaporation time and the volumetric heat transfer coefficient, so parameters will also be available for the actual condition, once they have been improved by taking into account the above variations.

A correlation relation for the description of single liquid droplets evaporation in an immiscible liquid is presented by the relation (5):

$$Nu = 0.121 \, Pe^{0.5} \tag{10}$$

Vorayos et al. in (2001) [9] studied ice thermal energy storage with direct-contact evaporator. The system consists of two cycles, basic chilled water and ice storage. The mathematical models for main components composed of compressor, condenser, expansion valve and water chilled direct-contact evaporator are developed and the system simulation is created. Evidently from the results, the simulation agrees well with experiments within 5 % error. Different options of the energy storage types, full storage, partial storage and demand-limited storage, have been considered. The simulation also indicates that the demand-limited storage design system is the most appropriate storage option for the selected office. Under this operating condition, the system can shift 39.3 % of peak electricity demand from on-peak period to off-peak period. Therefore, 33.8 % of electrical bill is saved compared to those of the conventional system.

The space cooling of the office is normally supported by conventional chiller unit of about 5 TR (approximately 18 kW_{th}). To modify the unit with the ITES system, another 2 TR (approximately 7 kW_{th}) refrigeration unit is used for ice storage unit. The schematic diagram of the air conditioning system with the ITES unit is shown in Fig. 19.
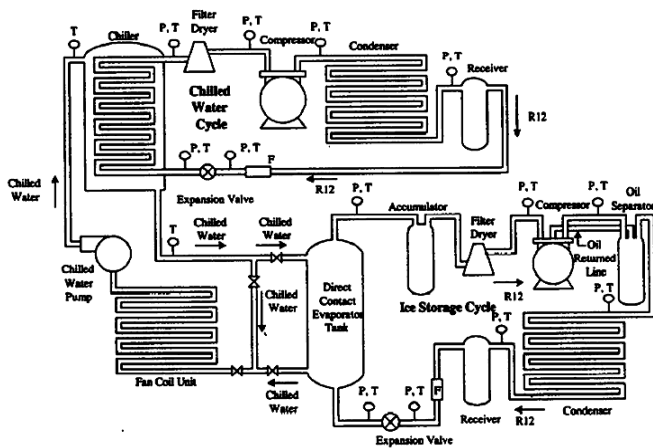

Fig. 19 Schematic diagram of the ice thermal energy storage system.

Table 8 the time used to generate ice and the amount of ice formed in the evaporator-storage tank. The results agree quite well with those of the experiments.

Mass of water in storage tank (kg)	m_r (kg/s)	N (rps)	Initial water temp. (°C)	Tan, h (°C)	Produced Ice (kg) (sim.)	Time (hr) (sim.)	Produced Ice (kg) (exp.)	Time (hr) (exp.)
250	0.077	11.8	18.0	29.2	250	3.66	212	3.59
250	0.100	11.8	16.5	30.2	250	3.11	209	3.23
300	0.066	11.8	15.0	28.5	300	5.01	272	4.98
300	0.100	11.8	15.4	26.8	300	3.67	269	3.62

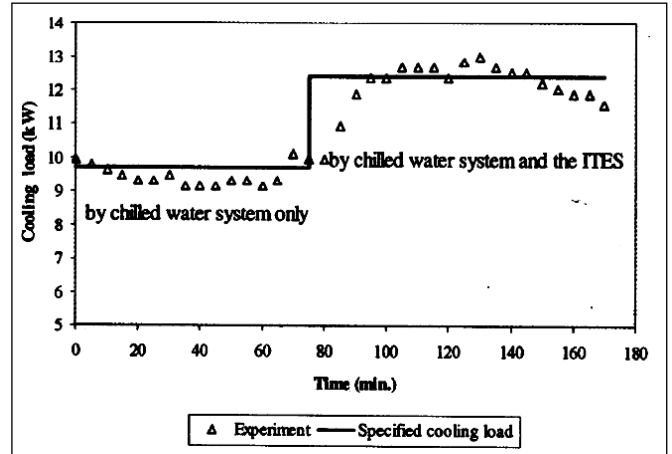**Notes:** sim. = for simulation,   exp. = for experiment.

Fig. 20 the using of Ice storage for cooling.

The following figures show the results of the COP with refrigerant mass flow rate (m_r) for the chilled water system and the storage ice system.
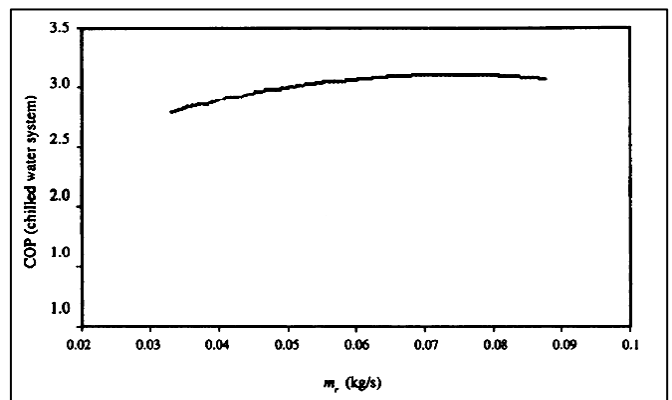

Fig. 21 the results of the COP with refrigerant mass flow rate (m_r) for the chilled water system.
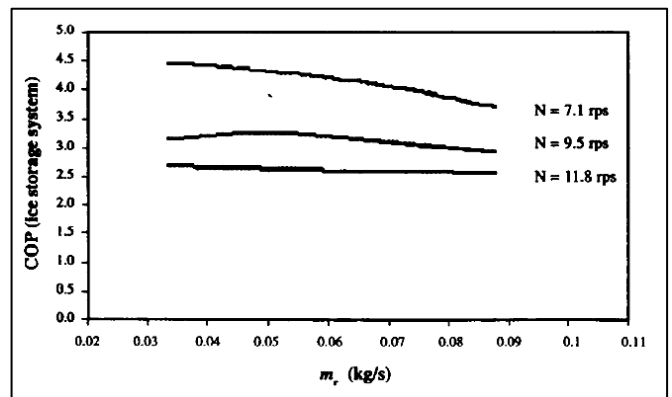

Fig. 22 the results of the COP with refrigerant mass flow rate (m_r) for the storage ice system.

Vuarnoz et al. in (2004) [2] studied important decreases of refrigerant amounts achieved by using secondary refrigeration fluids with direct-contact heat exchanger. Ice slurry is a two-phase fluid and thus, compared to single phase secondary refrigeration fluids, gives the advantage of the latent heat of fusion when the ice phase melts throughout heat exchange. Therefore, the challenges that the introduction of ice slurry as a common thermal fluid is facing are, in the first place, how to generate ice slurry in an efficient and ecological way. Optimal setup of a direct contact ice slurry generator requires studying the injection and the mechanisms of the evaporation of the refrigerant in the aqueous solution. The evaporation chamber is the main domain of our studies presented in this article. Some aspects of the development of the liquid-to-gas phase-change of the refrigerant, and of the liquid to solid phase-change of the water are presented in this article. Basic theory, velocity profiles achieved by Ultrasonic Doppler Method, and extracted values from measurements help to understand how to optimize the process of ice formation by an expanding jet of refrigerant in a vertical cylinder of water. The experimental setup for ice slurry generation as explained in the Fig. 23.
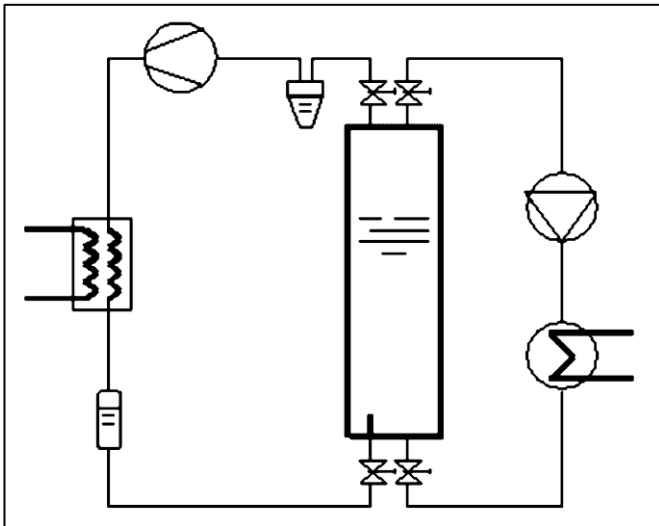

Fig. 23 Schematic drawing of the direct injection system.

In this vapor compression cycle, direct contact evaporation is applied. Technical differences from the conventional apparatuses are the evaporation chamber and the injection of refrigerant.

The injection is performed through a nozzle, which causes not only the expansion of the refrigerant but also the movement and turbulence of the mixture in the evaporation chamber. A tube in Plexiglas of 400 mm diameter was fixed 3 cm above the nozzle to concentrate the injected flux of refrigerant.

The refrigerant expands and evaporates inside the evaporation chamber at constant pressure and constant temperature (< 0 °C). The vapor rises through the contents of the vessel and the compressor absorbs it away. Throughout the evaporation, the latent heat of evaporation is withdrawn from the surrounding carrier fluid. At locations where this refrigeration effect leads to temperatures slightly under the freezing temperature of the aqueous solution, the water in the solution begins to freeze to small ice particles, which are suspended in the remaining unfrozen aqueous solution. This way, a specified amount of the water of the solution can be transformed into finely dispersed ice. The remaining aqueous solution has a higher concentration of freezing depressing agent and stays liquid. The applied measurement device for experimentally studying the injection is an Ultrasonic Velocity Profiler UVP-XW3. The positions of the UVP probes are detailed in following figure. The UVP measurements were performed separately for each height.

One way to explain the results of a UVP measurement is the color plot explained in the figure below. From this plot, the diameter, velocity and horizontal position of drabbles can be obtained. The following table shows average values determined from recorded information such as in the following figures. The velocity, size and dribble position along the ultrasonic beam are listed for the four heights where measurements were taken.

Table 9 the synthesis of mean values determined from data of Ultrasonic Doppler Method investigation.

Level	Z (m)	D (mm)	U (m/s)	X_{max} (mm)	f_{inj} (Hz)
1	0.5	22.2	0.366	- 3.9 / 4.5	0.737
2	0.8	26.6	0.432	- 12.4 / 10.8	3.119
3	1.1	23.7	0.448	- 17.4 / 16.1	0.758
4	1.4	24.9	0.397	- 21.6 / 18.7	1.4

The Ultrasonic Doppler Method has been applied to the process of ice slurry generation by direct injection of a refrigerant within an aqueous solution. Some theory of the physics included, such as the injection regime and the evaporation processes, has been shown. The main objective of this test has been to investigate the fluid dynamic behavior of evaporating refrigerant drops in an immiscible fluid and the approach taken has been to evaluate how suitable the UDM technique is for such examinations. The diameter, the velocity and the position of evaporating refrigerant drops were estimated from the results of Ultrasonic Doppler Measurements. The determined values agree well with numerical results. For better comparison with numerical simulation, enhanced studies of the initial conditions of the injected refrigerant reduction are needed.

6. Study bubbles formation and the effect of the hydrate layer on cold storage

Mori and Mori in (1989) [14] studied the physical process of forming gas hydrates in direct contact water. They used R12 vapor with adequate pressure. R12 flows into crystallized water, either liquid or vapors, consisting of three overlapping phases and evaporating before flowing out, cooling liquids into the crystalline and forming R12 hydrates as a cool storage medium. They observed that the hydrates appear in two different forms, with isolated layers forming in crystallization: one in the sediment particles at the bottom of the water phase and the other in the form of solid foam floating on the surface. Hydrate formation was discussed in each form. Fig. 24 shows the schematic of experimental refrigerator loop.

The important discovery of these experiments is that hydrate layers are based on two images. The layer on the bottom of the water / R12 has an agglomerated mortar form, while there is still an appropriate amount of liquid water in the crystalline to form the hydrate molecules. This feature is useful for heavy cold storage in a volume mask. In experiments, an increase in the number of hydrate molecules was achieved when the initial ratio of the thickness of the water to the total elevation on the liquid surface of water / R12 was more than 0.3.
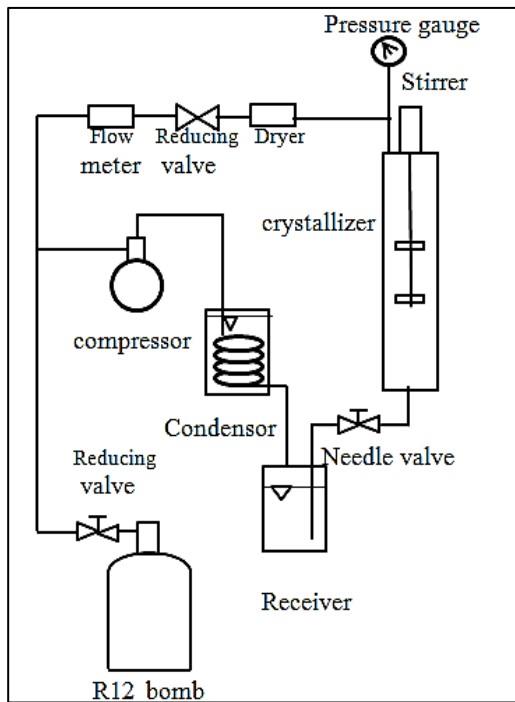
Fig. 24 Schematic of experimental refrigerator loop.

Therefore, it is better to equip some devices either to make the hydrate drop in the water phase or to get rid of the porous layer in the layer of density is greater, and therefore can store cold at a higher density.

It is possible to say that the experimental results obtained in this research using a small crystallization device through which the generalization of R12 is acceptable. For example, the size of the sub-cooling, the dimensional effect and the geometry of the crystallization device used, as well as the quality and purity of the refrigerant injected into the crystallization device may be. Nevertheless, we assume that the basic concept that we have reached through this process on the mechanisms of formation and structure of the hydrate layers is valid and that the data will be widely changed and will serve as a basis for further research on the storage mechanisms of gas hydrate cooling.

Mori and Mori in (1989) [15] studied evaporation by direct contact of gaseous hydrates within water, where molecules of different compounds are placed in hydrogen-related water molecules. That some CFCs, such as R11 (trichloroformachane, CC1, F) and R-12 (dichlorodifluoromethane, CC12F), form hydrates in exchange for heat and condensation, which can be found at temperatures up to Approximately 281.6 and 285.2 Kelvin, respectively (Davidson, 1973). The R-11 and R-12 hydrates were considered the most suitable for cold storage of residential air conditioning systems (Turn, 1984; Akia et al., 1987) to prevent the use of chlorofluorocarbons.

R-134 (1, 1, 1, 2-tetrafluoroethane, CF, CH, F) is currently an alternative to R-12 and has been replaced by conventional refrigeration and air-conditioning equipment. However, it was not confirmed that R-134a could be a gas hydrate that could be used for cold storage. In this work, we wanted to find out if R-134a could form gas hydrates, and determine the highest temperature they could be, with reasonable accuracy for practical purposes. The temperature of the quaternary point, where hydrates can be formed, for R-134a in both its vapor and liquid state, and water in the liquid state.

It has been observed that the R-134a gas hydrates are formed in the crystalline in the same way as R-134a hydrates when the crystal hydrate is almost completely stored. The circulation was then stopped and the crystallization was left to be heated by laboratory air, which is reflected in the slow degradation of the hydrate to R-134a in the liquid, vapor and water state of the liquid state. At the same time, the temperature and pressure in the crystal showed stable values until the decomposition is complete. These stable values for temperature and pressure were considered to be similar in the quadratic point, with values of 283.1 ± 0.3 K and 0.415 ± 0.009 MPa, respectively. The specific quadratic point on the pressure chart is plotted with the temperature in the Fig. 25 to compare it with a curve representing the total sum of the designed steam pressure for R-134a and water.
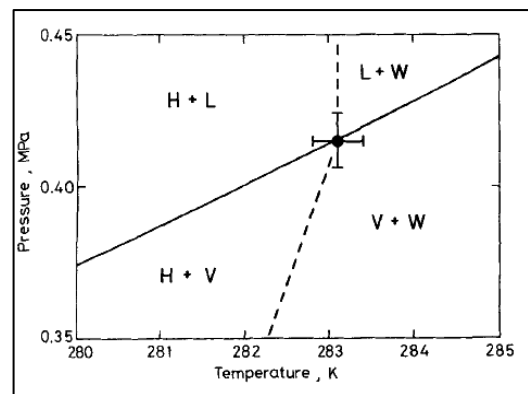

Fig. 25 The Phase diagram for R-l34a/water system.

R-134a vapor pressure was determined through the relationship presented by Piao et al. (1988) according to their practical data. For water vapor pressure, the information in JSME (1983) was used. It is known that the quartile point specified in this experiment falls within the ambiguous places of measurement on the curve and is uniform with the R-134a vapor pressure information obtained from Piao et al.

Mori and Isobe in (1991) [16] presented a physical model for the mechanism of formation of gas hydrates during evaporation by direct contact within organic coolant and water. Hydrate is assumed to be formed on the cover of each refrigerated bubble, due to the bonding of the water molecules and the cooling bubble, thus turning the bubble into a hydrate balloon. An arithmetic scheme is designed to predict the evaporation and composition of the refrigerant in each hydrate, based on the balance of heat transferred from water to the bubble, evaporative heat, and the heat of hydrate formation.

The problem is determined numerically, using an exact finite-difference scheme, for the volume of a bubble, V, and for the volume of a hydrate in the bubble, V_h, changing with the slip of time since the simultaneous nucleation's of vapor and hydrate phases.

Figure 26 shows predicted changes of V, V_h and ξ_h with time slip next to the nucleation's of vapor and hydrate in a CFC-12 drop of 1.5 mm primary diameter, a = 0.05 kg/m^3-s, b = 1.0, T_c = 275 K and ΔT_{cs} = 2.0 K unless oppositely remarked in diagrams.
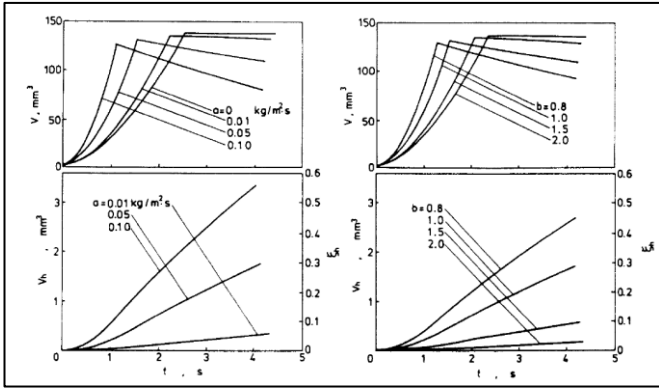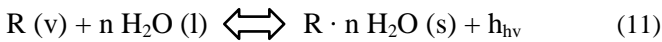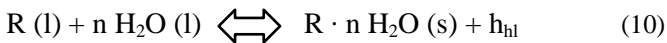
Fig. 26 Predicted variations of V, V_h and ξ_h with time lapse after the nucleation's of vapor and hydrate in a CFC-12 drop of 1.5 mm initial diameter, a = 0.05 kg/m³-s, b = 1.0, T_c = 275 K and ΔT_{cs} =2.0 K, unless otherwise noted in graphs.

The primary part we expect the model gave above to play is to present a clear situation of the evaporation/hydrate-formation method in a direct-contact evaporation cool-storage facility.

We assume the model to be confirmed in this respect. As a tool for divining quantitatively the hydrate production, however, the model may be too crude and may require further sophistication.

Besides, the great uncertainty in the rate of the chemical reaction Eq. (10) or Eq. (10) presents a serious difficulty in utilizing the model as such a device. A better understanding of the reaction properties and test observations directly relative to the predictions are wanted.

$$R \text{ (l)} + n\ H_2O \text{ (l)} \Longleftrightarrow R \cdot n\ H_2O \text{ (s)} + h_{hl} \qquad (10)$$

$$R \text{ (v)} + n\ H_2O \text{ (l)} \Longleftrightarrow R \cdot n\ H_2O \text{ (s)} + h_{hv} \qquad (11)$$

7. Studying the dimensionless relation of the Direct-Contact heat exchanger

Kiatsiriroat et al. in (2003) [7] studied the heat transfer properties of a direct contact evaporator. A refrigerated two-phase refrigerant (R12 or R22) is injected inside the water put in a storage tank to exchange heat with the water directly. The water temperature is decreased to the freezing point, and ice could be formed. The lumped model is utilized to predict the water temperature, and it is determined that this model can predict the water temperature very quiet. A relationship that describes the dimensionless parameters, such as Stanton number, Stephan number, Prandtl number, and pressure ratio, is also developed.

Figure 27 the experimental organization which consists of a direct contact evaporator, a dryer unit, a compressor, a condenser, a receiver, and an expansion valve. The direct contact evaporator is a stainless steel storage vessel with 30 cm diameter and 110 cm height. The refrigerant from a receiver is injected within the expansion valve to decrease the pressure and temperature.
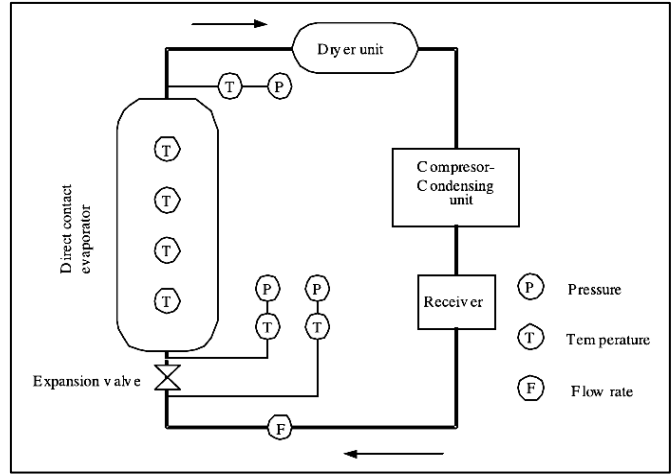

Fig. 27 Schematic diagram of the experimental apparatus.

The parameters affecting the heat transfer of the direct contact evaporator could be arranged into dimensionless parameters that could be arranged in terms of Stanton number, Stephan number, and Prandtl number, where:

$$St = \frac{U_V\ V}{(\dot{m}\ C_p)r} \qquad (12)$$

$$Ste = \frac{C_{pw}(T_w - T_{ri})}{\lambda_w} \qquad (13)$$

$$Pr = \frac{C_p\ \mu}{k} \qquad (14)$$

St is Stanton number, Ste is Stephan number and Pr is Prandtl number. The dimensionless group could be expressed as:

$$St = Ste\ Pr^{0.25} \left(\frac{P}{P_a}\right)^{-1} \qquad (15)$$

Figures 28 and 29 show the relation of the dimensionless parameters and the comparison of St with the experimental data.
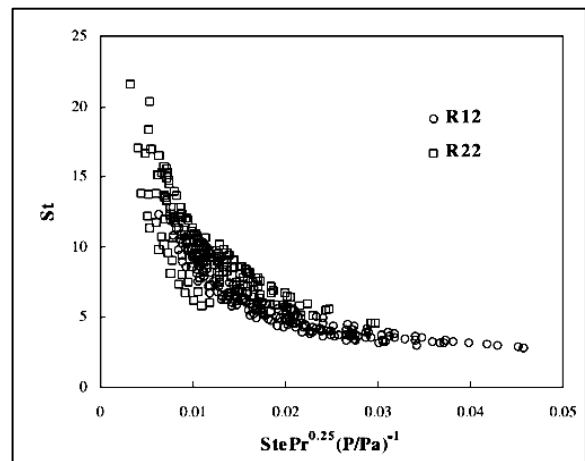

Fig. 28 Relation of the dimensionless parameters.

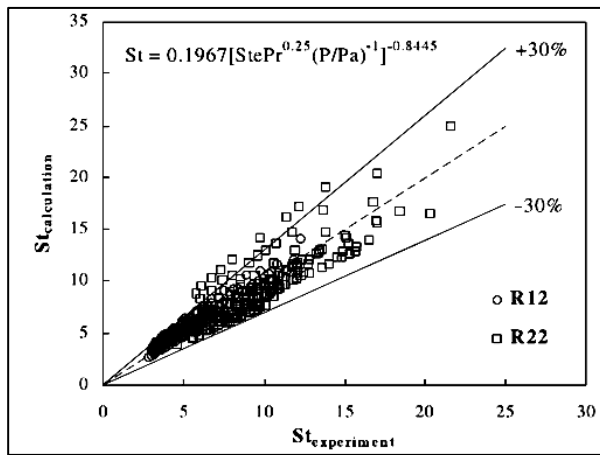$$St = 0.1967[StePr^{0.25}(P/Pa)^{-1}]^{-0.8445}$$

Fig. 29 Comparison of St with the experimental data.

The conclusion of this experiment the direct contact heat transfer method with the injection of refrigerant provides a high heat transfer rate. The lumped model can be modified to predict the temperature of the water throughout the sensible heat period and the quantity of ice throughout the latent heat period. The relationship of the dimensionless parameters is represented, and it can be utilized to predict the experimental value very quiet.

8. Conclusions

Through previous research and studies in the field of heat transfer by direct contact between the cooling medium and water, we can summarize our conclusions in the following points:

1. The direct contact heat transfer method is effective in the speed of heat transfer and the speed of reaching the required design degree.
2. The evaporator piping problems are eliminated from corrosion and heat resistances.
3. At the beginning of operation, the compressor temperature rises as a result of the hot refrigerant coming from the evaporator, gaining the high temperature of the water, and its temperature gradually decreases with time.
4. This method can be used in applications of industrial ice production and heat storage.
5. Consider the use of insoluble and dissolving liquids in evaporated water.
6. The heat transfer is mainly dependent on the ability of the surface of the coolant bubbles to depend on the heat from refrigerant.

References

[1] K. Stephan and K.-D. Stopka, "Direct contact heat transfer during evaporation of immiscible liquid mixtures", International Journal of Refrigeration, Vol. 4, No. 2, pp. 91-96, 1981.

[2] Didier Vuarnoz, D. Ata-Caesar, Osmann Sari and Peter William Egolf, "Ultrasonic Measurements in Ice Slurry Generation by Direct Contact Evaporation", Fourth International Symposium on Ultrasonic Doppler Method for Fluid Mechanics and Fluid Engineering (ISUD-4) at: Sapporo, Japan, 6-8 September 2004.

[3] T. Kiatsiriroat, P. Siriplubpla and A. Nuntaphan, "Performance Analysis of a Refrigeration Cycle Using a Direct Contact Evaporator", International Journal of Energy Research, Vol. 22, No. 13, pp. 1179-1190, 1998.

[4] Raksit Thitipatanapong, "An Experimental Study of Direct Contact Ice Slurry Production System", M. Sc. Thesis in Mechanical Engineering, Sirindhorn International Institute of Technology, Thammasat University Thailand, May 2004.

[5] Ammar A. Ojimi, Hussien S. Sultan and Amani J. Majeed, "Experimental Study of Direct Contact Evaporation Refrigeration System using R-12", Thi_Qar University Journal for Engineering Sciences, Vol. 8, No. 2, 2017.

[6] G. P. Celata, M. Cumo, F. D'annibale, F. Gugliermetti and G. Ingui, "Direct contact evaporation of nearly saturated R114 in water", International Journal of Heat and Mass Transfer, Vol. 38, No. 8, pp. 1495-1504, 1995.

[7] T. Kiatsiriroat, S. Vithayasai, N. Vorayos, A. Nuntaphan and N. Vorayos, "Heat transfer prediction for a direct contact ice thermal energy storage", Energy Conversion and Management, Vol. 44, No. 4, pp. 497-508, 2003.

[8] Raksit Thitipatanapong, Bundit Limmeechokchai, and Supachart Chungpaibulpatana, "Investigation of Direct-Contact Heat Exchanger for Ice Slurry Production", Regional Conference on Energy Technology Toward a Clean Environment, The Joint Graduate School of Energy and Environment at: Thailand Volume: 2nd, 2003.

[9] N. Vorayos, T. Kiatsiriroat, and A. Nuntaphan, "Feasibility of using ice thermal energy storage with direct contact evaporation in an office building", Asian j. Energy Environ, Vol. 2, Issue 3-4, pp. 199-231, 2001.

[10] Yaokang Zhang, Lin Su, Kaijun Dong, Tengqing Liu, "Experimental study of ice slurry production system using direct contact heat transfer of RC318 and water in a horizontal pipe", Energy Procedia, Vol. 158, pp. 4495-4501, 2019.

[11] Raksit Thitipatanapong and Bundit Limmeechokchai, "The Direct Contact Heat Exchanger: Experiences on Ice Slurry Production", Joint International Conference on Sustainable Energy and Environment (SEE). 1-3 December 2004, Hua Hin, Thailand, 2004.

[12] Najim A. Jassim and Fatimah A. Abdulkhaleq, "Performance Evaluation of Three Phase Spray Direct Contact Heat Exchanger", Iraqi Journal of Chemical and Petroleum Engineering, Vol. 15, No. 4, pp. 37-45, 2014.

[13] F. Isobe and Y. H. Mori, "Formation of gas hydrate or ice by direct-contact evaporation of CFC alternatives", International Journal of Refrigeration, Vol. 15, No. 3, pp. 137-142, 1992.

[14] T. Mori, Y. H. Mori, "Characterization of gas hydrate formation in direct-contact cool storage process", International Journal of Refrigeration, Vol. 12, No. 5, pp. 259-265, 1989.

[15] Yasuhiko H. Mori and Tatsushi Mori, "Formation of Gas Hydrate with CFC Alternative R-134a", AIChE Journal, Vol. 35, No. 7, pp. 1227-1228, 1989.

[16] Yasuhiko H. Mori and Fumiho Isobe, " A model for gas hydrate formation accompanying direct-contact evaporation of refrigerant drops in water", International Communications in Heat and Mass Transfer, Vol. 18, No. 5, pp. 599-608, 1991.

Nomenclature

Symbol	Quantity	Symbol	Quantity
A	Area	Q_c	Water volumetric flow rate (m³/sec)
Ab	Droplet surface area	Q_{SE}	Stored refrigerated energy (MJ)
C.O.P.	Coefficient of performance	R	Refrigerant
CP	Specific heat	r	Equivalent spherical diameter ratio D/D_o
Do, D	Initial and instantaneous equivalent spherical diameter	RD	Droplet radius of the two-phase bubble (m)
dl	Drop liquid	Re	Reynolds number
dv	Volume change	r_r, r_w	Evaporation enthalpies (refrigerant, water)
h	Enthalpy (J/kg)	s	Parentheses mean solid state
Hb	Volumetric heat-transfer Coefficient.	S_t	Stanton number
h_c	The heat transfer coefficient for continuous phase (water).	S_{te}	Stephan number
K	Thermal Conductivity	ΔT_m	Logarithmic mean Temperature
l	Parentheses mean liquid state	T_r, T_w	Temperatures (refrigerant, water; 1-inlet, s-saturation)
L_d	Latent heat of vaporization of dispersed phase.	T_m	Thermodynamic temperature of mixing difference (°C)
M	Mass (kg)	ΔT	Temperature difference between continuous and dispersed phases
m_d	Mass flow rate of dispersed phase (kg/s)	Δt_{ice}	Time duration for producing ice (s)
m_v	Mass flow rate	U	Velocity (m/s)
m_r^g, m_w	Mass flow rate (refrigerant, water; g-gaseous, liquid)	UA	Overall heat loss coefficient and area (W/K)
MTD	Main temperature difference (°C)	UDM	Ultrasonic Doppler measurements
Δm_w	Evaporating water mass flow (Kg/s)	U_v or h_v	Volumetric heat transfer coefficient (w/m³. K)
n	Drift-flux model parameter	v	Parentheses mean vapor states
nb	Droplet number density	V_{od}	Injected volume (cm³)
Nd	Number of droplets (1/m³).	X	Vaporization ratio
Nu	Nusselt number	Z	Vertical coordinate (m)
Pr	Prandtl number	λ	Latent heat of freezing (J/kg)
Q	Heat flux (watt)	α, β, γ, δ	Constants